TOWARD SMART CONTROL OF SEPARATION AROUND A WING
-Active Separation Control System part 2-

Akira NISHIZAWA and Shohei TAKAGI
Japan Aerospace Exploration Agency, Chofu, Tokyo, 182-8522

Hiroyuki ABE, Takehiko SEGAWA, and Hiro YOSHIDA
National Institute of Advanced Industrial Science & Technology, Namiki, Tsukuba, 305-8564

Abstract

Leading-edge separation on a wing model was automatically controlled by a closed-loop system which was composed of a flow-direction discriminator, a controller and disturbance actuators. The discriminator made use of MEMS technology works well as a stall warning device. The separation was prevented by exciting the shear layer using periodic blowing and suction. A computer controlled these elements by using a simple algorithm. Results of the demonstrations of the integrated control system for pitching motion of the wing showed the effectiveness of this system toward the smart wing.

1. Introduction

Control of flow separation has been obviously one of the most noticeable fluid engineering subjects. The potential advantages of applying separation control are expected to be greatly useful for various systems such as air, land, and sea vehicles; turbomachines; diffusers; and a variety of other technologically important systems involving fluid flow (Gad-el-Hak 2000). There are large numbers of investigations on actuation methods of control of flow separation. Ahuja and Burrin (1984) and Hsiao et al (1990) used acoustic excitation for control. Neuburger and Wygnanski (1987) used vibrating ribbon to delay separation. By using synthetic jet technique, Glezer's group (1999, 2001) has carried separation control and virtual-shaping of airfoils. For practical applications in civil aircrafts, the attempting of pneumatic flow control to high-lift systems is predicted to have the greatest impact by McLean et al (1999). In such a case, feedback control methods may not necessarily be required, however, other new types of air vehicles such as unmanned aerial vehicles and micro aerial vehicles have come to be in the limelight as application objects using flow control recently. As stated by Greenblatt and Wygnanski (2000), these aerial vehicles possibly give many new subjects involved flow control. McCormick et at (2001) pointed out that packaging of a self-contained actuator inside the confined leading edge of the airfoil represented a significant challenge. Establishing a compact control system which can be installed in a small wing seems to be more important.

One of the goals in the MEMS subgroup is to establish the basis of smart, i.e. feedback and/or feedforward, control system of flow separation around wings. So far, this subgroup has investigated the possibility of thermal multi-sensors as separation detector on circular cylinder body and airfoil (Takagi et al. 2001). Takagi et al. (2002) and Nishizawa et al. (2003) investigated the techniques of separation-detection and separation-prevention with the use of a new small surface sensor (Ozaki et al, 2000), which has been originally developed for a model of wind receptor hairs of insects. Abe et al (2001) are studying micro jet vortex generator (MJVG) instead of former solid fin type VGs. The present study aims to integrate the separation detector, actuator and control algorism which have been studied in our group and to apply them to an actual wing model.

2. Experimental Apparatus

2.1 Wind tunnel and wing model

A suction type of wind tunnel was used for the present experiments. The maximum flow speed is 18 m/s. The turbulence intensity of the free stream is less than 0.3% at a free stream velocity of 10m/s. A schematic view of the test section is shown in Fig.1. The size of test section is 1500mm in length, 600mm in height, 300mm in width. A NACA0015 wing model was placed at the center of test section. Its chord length, c, is 400mm, width, b, is 300mm and aspect ratio, b/c, is 0.75. The angle of attack, α, is set by a rotary table. The free-stream velocity, U_∞, is defined as the velocity where the Pitot tube is located. The experiments were conducted at U_∞=10m/s and the Reynolds number, R_e, based on the chord length and U_∞ is nominally 2.8×10^5. Uncertainty of the Reynolds number due to ambient temperature drift is kept within ±8%. In the coordinate system, *x* and *z'* are the chord wise and vertical direction respectively.

Figure 2a shows the picture of smart wing model. The Plexiglas-made model has two thin plates near the

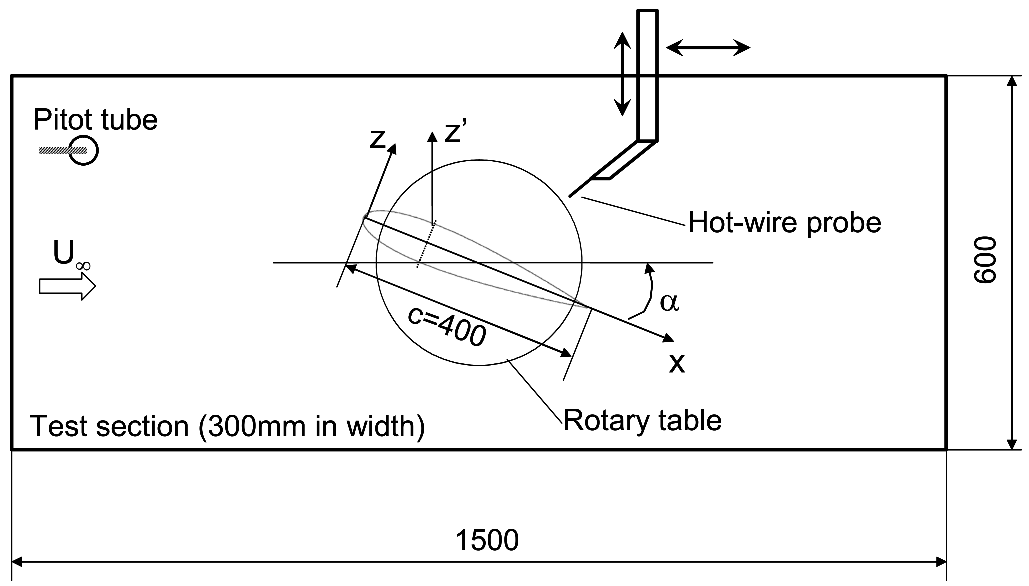

Fig.1 Experimental setup (unit:mm).

both sides to eliminate the influence of the boundary layers developed on the test section wall. Three loud speakers were installed at 90mm spacing in spanwise direction as shown in Fig.2b. Five 0.5 mm diameter holes were drilled at the leading edge (*x*/*c*=0) at 10mm spacing in spanwise direction for each speaker. These

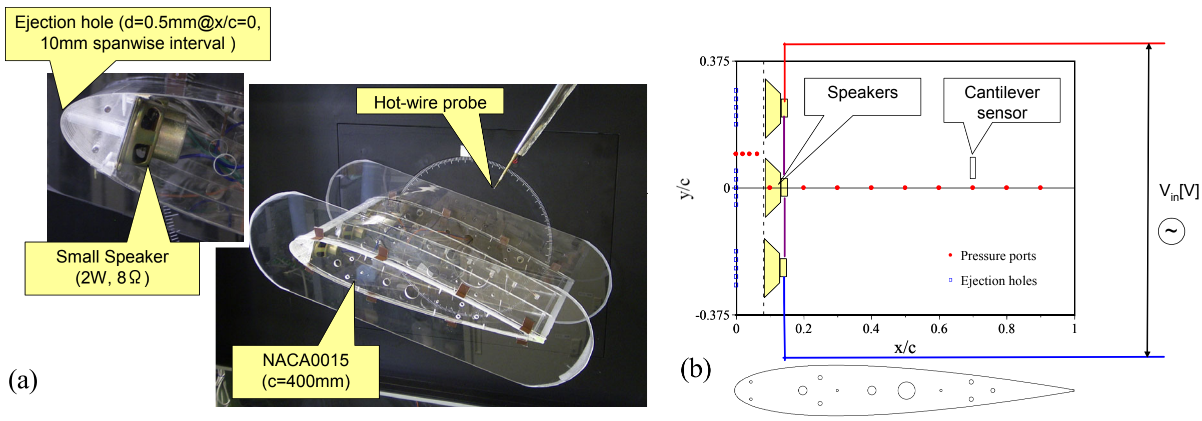

Fig.2 NACA0015 wing model. (a)pictures, (b)schematic views

speakers are connected in series. Pressure ports are located on the center line of the upper surface at 40mm spacing except near the leading edge.

2.2 Separation detector

A cantilever sensor (CS) as shown in Fig.3, was used as a reverse-flow detector. The CS was installed at x/c=0.7 off the centerline. This sensor was made use of MEMS technology and consisted of five independent cantilevers. They are 0.23mm in width and 0.01mm in thickness. Each element has a strain gauge at the root near the base so as to interpret flow direction: the sensor output for reverse flow indicates the negative sign, and vice versa. In this experiment, the longest cantilever was used together with an amplifier (TEAC Model SA-59) with an excitation voltage of ±0.6V and a DC gain of 2000. The effect of thermal drift due to variation of the ambient temperature was eliminated by observing the output at no wind before and after the measurements. However unavoidable offset is retained within ±3mV through the measurements. More details on the gauge are given by Ozaki et al. (2000).

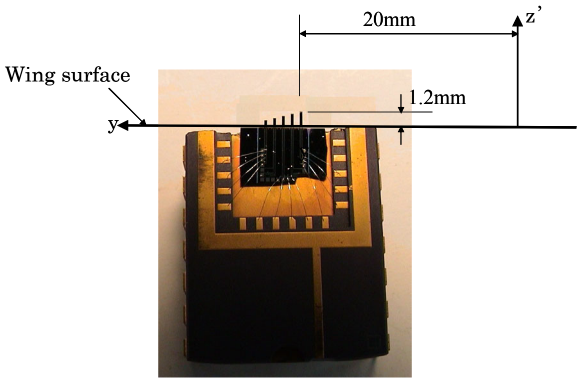

Fig.3 Cantilever sensor (Ozaki et al. 2000).

2.3 Control System

To examine an active control of the leading edge separation, the boundary layer on the wing surface was excited by periodic disturbance at the leading edge. As mentioned above, three small speakers which were applied sinusoidal voltage through a function generator and an AC amplifier were used as actuators. Figure 4 shows an example of time trace of the hot-wire output measured above the hole for no wind at disturbance frequency of 100Hz. The trace indicates that the strong blowing and weak suction repeated at the period of the speaker oscillation. Since the hotwire cannot detect the flow direction, blowing and suction phases are assumed. The magnitude of the disturbance, V_j', is defined by the root mean square of the fluctuating velocity. Parametric study of the disturbance frequency and magnitude enabled us to optimize the control condition.

The closed-loop control system consisted of three simple procedures as shown in Fig.5: acquisition of CS output, discrimination of the flow direction and excitation of the boundary layer. For the discrimination of the reverse flow, time averaged voltage of CS output was used: if it is positive the speaker is not driven and vice

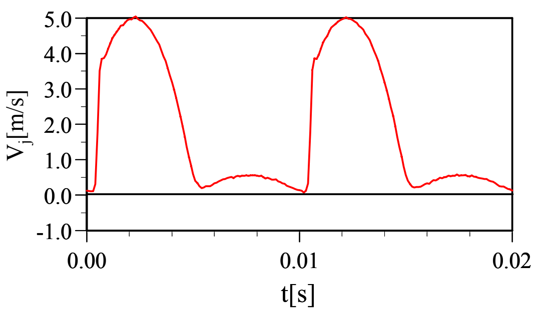

Fig.4 Time trace of the hot-wire output, V_j, measured above the ejection hole (z'=0.5mm) for no wind at f=100Hz.

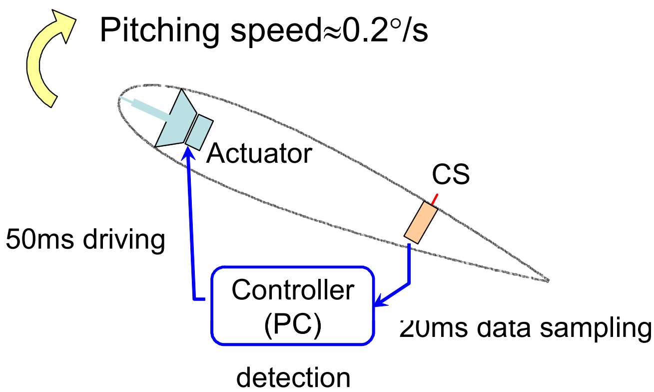

Fig.5 Schematic view of the control system.

versa. The durations of acquisition and excitation can be independently adjusted. The durations of 20ms for the acquisition and 50ms for the excitation were used in the present experiments.

2.4 Data acquisition and analysis

Profiles of the mean and fluctuating velocities in flow around the wing were measured by a conventional constant-temperature hot-wire anemometer and a single-wire probe. The anemometer output was analogously linearized using a pressure transducer connected to a Pitot static tube in uniform flow. The hot-wire sensor mounted on a 2-D traversing mechanism was automatically moved by a computer. Time averaged C_p distributions were measured by a SCANIVALVE and a high sensitive pressure transducer. The Pitot static pressure, p_s, was used as the reference pressure in calculating the $C_p=(p-p_s)/(p_t-p_s)$, where p and p_t are the surface pressure of the model and the total pressure of Pitot tube respectively. The C_p distributions on upper surface in negative angle of attack were substituted for ones on lower surface in positive angle of attack.

The outputs from the anemometer, pressure transducer and a separation detector acquired by 16 bit A/D board installed in the computer. The uncertainty of velocity measurements is ±2% of the local velocity. Lift coefficient, C_L, was calculated by integration of the interpolated C_p distributions on both surfaces. The uncertainty of C_L is kept within ΔC_L =±0.05.

3. Result and discussion

3.1 Characteristics of basic flow

Figure 6 shows the streamwise variation of free-stream velocity and the boundary layer profile at x/c=0.3 for α=0°. The flow is highly accelerated around the wing, indicating that the blockage effect of the wing on the uniformity of the free stream is not negligible in the present experiments. For this reason, C_p distributions are

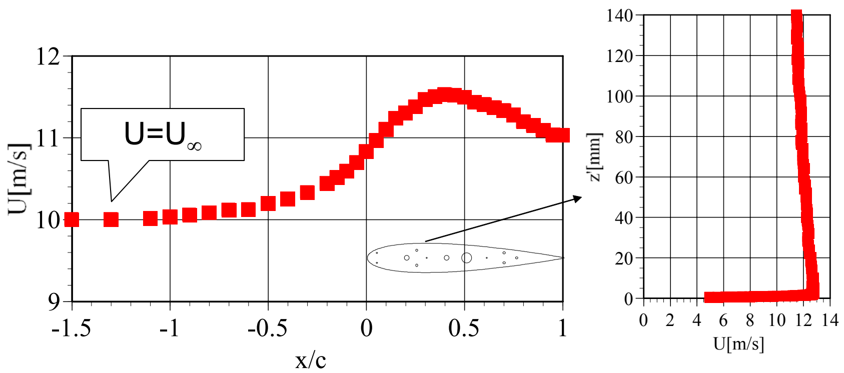

Fig.6 Velocity profiles at α=0°. (a) Streamwise distribution of the free-stream velocity at z=170mm and y=0, (b) vertical profile of the mean velocity at x/c=0.3 and y=0.

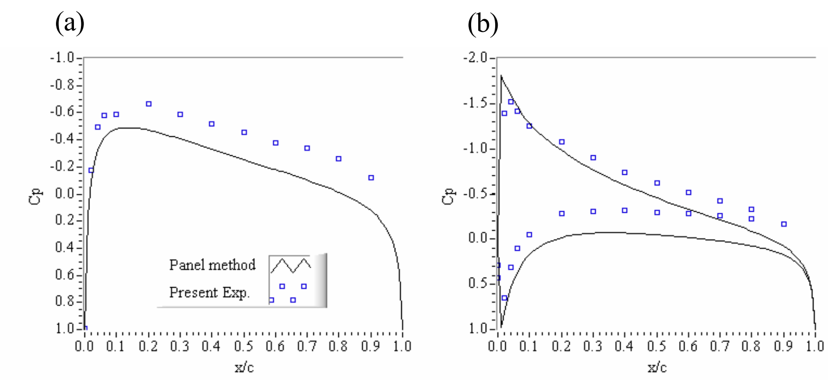

Fig.7 C_p distributions at (a) α=0° and (b) α=5°.

not in agreement with theoretical ones calculated by panel method as shown in Fig.7. The purpose of this study, however, is to establish the active control system rather than to investigate the flow field around a NACA0015 wing. Figure 8 shows the C_L distribution for various angles of attack without any separation control. These plots indicate that the stall angle is about 19 degree. Generally, two dimensional NACA0015 wing has much smaller angle of stall. This delay of stall seems to be due to very low aspect ratio of only 0.75. Inspite of these imperfect conditions, the effects of control system on the lift can be verified as described below.

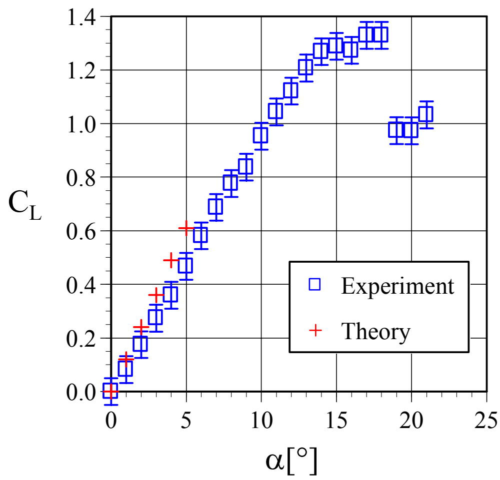

Fig.8 C_L distributions for various angles of attack.

3.2 Static control by a roughness element

Figure 9 shows the comparison between natural case and the case that the flow was disturbed by a 0.7mm diameter circular cylinder placed on the surface near the leading edge. The streamwise location of roughness element was varied from x/c=0.0 to 0.075. For the location of x/c=0.05 and 0.075, the roughness has no effect on the C_L distribution. The roughness located x/c=0.0 or 0.025 enhances the stall however the C_L took larger values than the natural case after the stall. These results reveal that the disturbance should be introduced near the leading edge to affect flow around the wing. Consequently, the periodic disturbance was decided to be introduced from the leading edge.

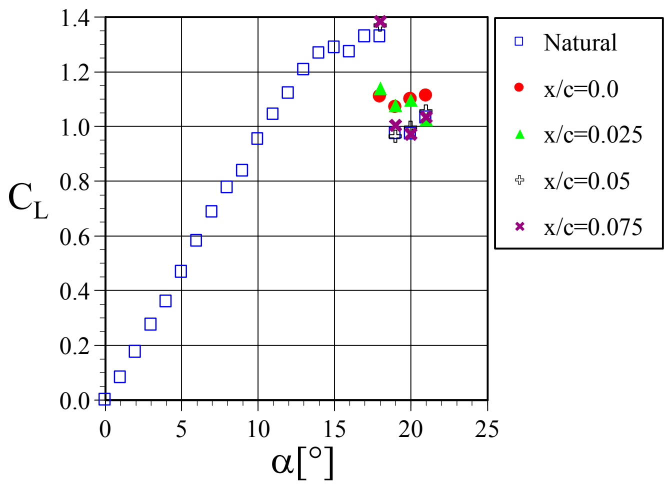

Fig.9 C_L distributions for various streamwise locations of a roughness element.

3.3 Active control by periodic disturbances

Figure 10 shows C_L distributions for variation of the disturbance magnitude and frequency. As shown in Fig.10a lager magnitude of the disturbance brings better effect on the lift recovery but the increment of magnitude finally results in saturation of the effect. On the other hand, the lift recovery effect does not depend

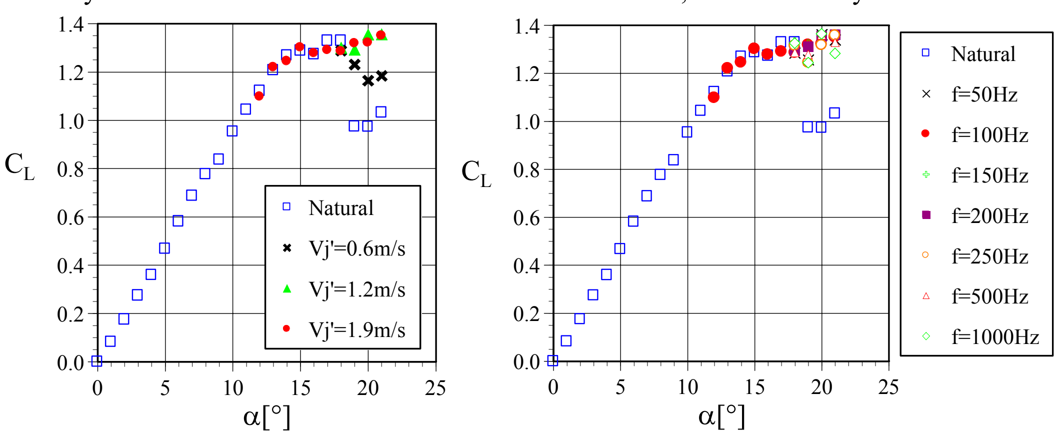

Fig.10 C_L distributions for various control conditions. (a) magnitude dependency at constant frequency of f=100Hz. (b)frequency dependency at constant magnitude of V_j'=1.9m/s.

on the frequency as shown in Fig.10b. In all cases for the frequency and magnitude, the active excitation method has no negative effect as seen in Fig.9. Because of the results for parametric study of frequency showed no difference, all of the following results are represented with the case of f=100Hz and V_j'=1.9m/s.

Figure 11 shows C_p distributions at α=20°. The plot for natural state looks almost flat on the upper surface indicating that the flow separated from the leading edge. For the case with active control, the C_p distribution on the upper surface has clearly recovered. These results indicate that the present control method is effective for stall due to leading edge separation. Figure 12 shows the profiles of velocities and turbulence intensities in the flow on the upper surface at x/c=0.7 and α=20°. The large-scale reverse flow seems to occur in the range of 0<z'<100mm for the natural case since the velocity is increased toward the wall. When the control is applied the velocity becomes to decrease monotonically toward the wall and the thickness becomes thinner, implying that the reverse flow is prevented by the control. Figure 13 directory shows this behavior. For natural case, the cantilever sensor output is always negative in Fig.13a, meaning that the flow is reverse, while the averaged sensor output becomes almost positive in Fig.13b for the controlled case. These results support the result by hot-wire measurements.

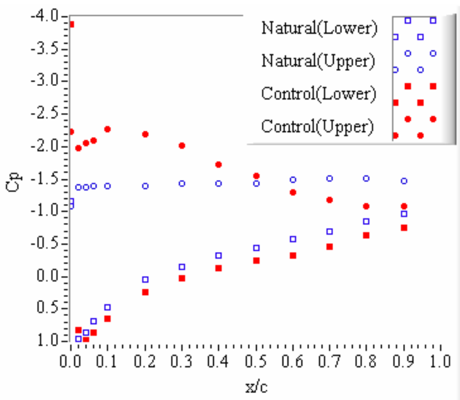

Fig.11 C_p distributions at α=20°. Control conditions are f=100Hz and V_j'=1.9m/s.

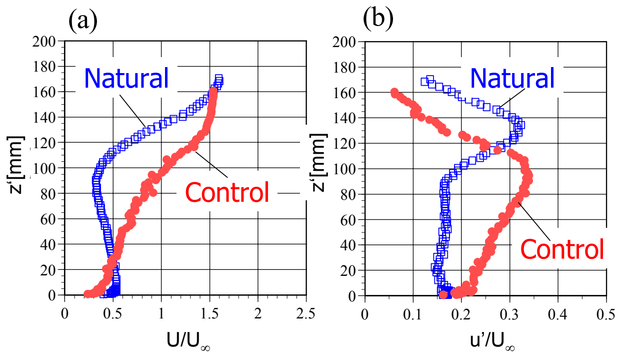

Fig.12 Profiles of (a)mean velocity, U, and (b)turbulence intensity, u', at α=20° and x/c=0.7.

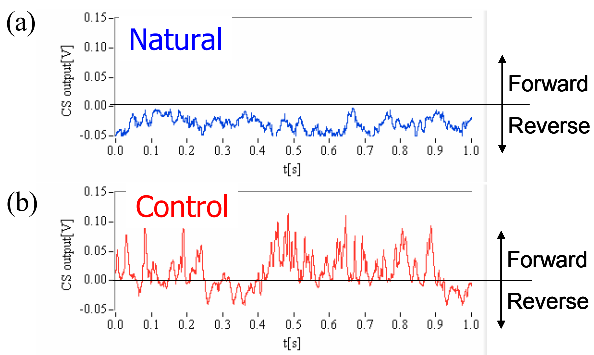

Fig.13 Instantaneous waveforms of Cantilever sensor output at α=20° and x/c=0.7. (a)Natural, (b)Control.

3.4 Demonstration of closed-loop control system

To demonstrate the automatic control system it was operated when the angle of attack was continuously changed by the rotary table at constant speed of about 0.2°/s. Figure 14 shows the time traces of CS output signal and speaker driving pulse in both cases with and without control. In case of the natural state, the CS output decreases with increase of the angle of attack and the reverse flow appears before the stall angle of α=19°. Needless to say, the first appearance of the reverse flow depends on the streamwise location of the CS. Although the location was not optimized yet in the present study, the CS works well as a warning device of the stall. When the control system is operated the speaker driving pulse is generated by detecting the reverse flow. The flow direction, however, does not change to forward up to the stall angle. After the stall angle, this system controls

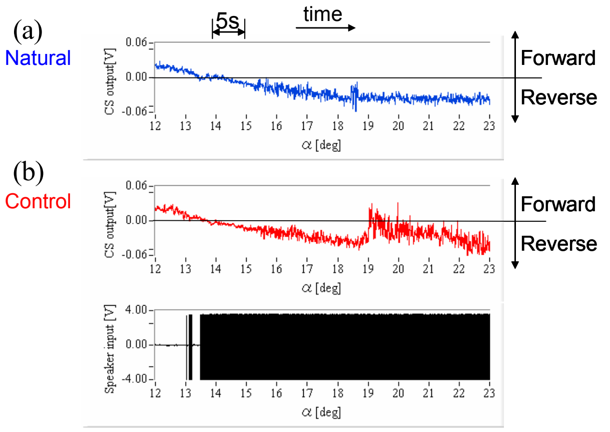

Fig.14 Demonstration of the control system for the pitching motion of the wing. (a) CS output without control, (b) CS output and speaker driving pulse with control.

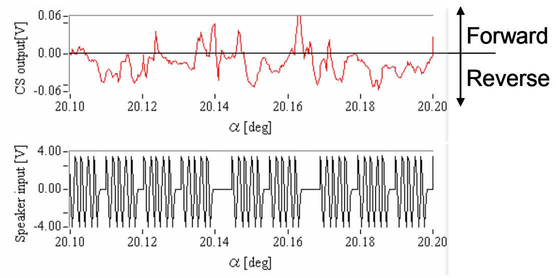

Fig.15 Extended waveforms of Fig.14(b).

the reverse flow well. Figure 15 shows the extended waveforms of Figs14b and c. The speaker is driven when the flow direction is reverse while it is not driven when the flow direction is forward, indicating that the automatic detection and control system works well even for short-time flow phenomenon.

4. Concluding remarks and near future plan

In the present study, the active separation control system developed for the simple flow field in the previous work was applied to a wing model. The system is composed of the flow direction sensor, the actuator which excites the separated shear layer and the computer controlling these elements. The discriminator made use of MEMS technology works well as a stall warning device. The system integration was established for the wing model and the smart control system was demonstrated for the pitching motion of the wing. It is verified that the present control system can prevent leading edge separation and delay the stall.

Although the present system employed the simple actuator which generates periodic blowing and suction, they can be easily replaced by the new actuators developed by coauthors in AIST. By using their micro jet vortex generators it is expected that the control system can be applied to the cases of higher Reynolds number and give birth to higher lift.

Acknowledgements

An air-flow sensor used as separation detector in this study was given by courtesy of Professor Isao Shimoyama, Department of Mechano-Informatics, the University of Tokyo. The authors would like to express their appreciation.

References

Abe, H., Segawa, T., Matsunuma, T., Yoshida, H., 2001, "Vortex generator composed of micro jet array for flow separation control", *Proc. 2nd Symp. Smart Control of Turbulence*, Univ. Tokyo, March 4-6, pp.117-120.

Abe, H., Segawa, T., Matsunuma, T., Yoshida, H., 2001, "Micro jet vortex generator for active control of flow separation", *Proc. International Conference on Power Engineering*, Oct.8-12, 2001, Xi'an China.

Ahuja, K.K., Burrin, R.H., 1984, "Control of flow separation by sound", *AIAA paper*, 84-2298.

Chatlynne, E., Rumingny, N., Amitay, M., Glezer, A., 2001, "Virtual aero-shaping of a Clark-Y airfoil using synthetic jet actuators", *AIAA paper*, 2001-0732.

Gad-el-Hak, M., 2000, *Flow control*, Cambridge Univ. Press.

Glezer, A., 1999, invited lecture, "Shear flow control using fluidic actuator technology", invited lecture in the *1st Symposium on Smart Control of Turbulence*, Dec.2-3, 1999, Tokyo, pp.39-45.

Greenblatt, D., Wygnanski, I.J., 2000, " The control of flow separation by periodic excitation", *Progress in Aerospace Sciences*, 36, pp. 487-545.

Hsia, F-B., Liu, C-F., Shyu, J-Y., 1990, "Control of wall-separated flow by internal acoustic exciteation", *AIAA J.* 28(8), pp.1440-1446.

McCormick, D.C., Lozyniak, S.A., MacMartin, D.G., Lorber, P.F., 2001, "Compact, high-power boundary layer separation control actuation development", *ASME paper* FEDSM2001-18279.

McLean, J.D., Crouch, J.D., Stoner, R.C., Sakurai, S., Seidel, G.E., Feifel, W.M., Rush, H.M., 1999, "Study of the application of separation control by unsteady excitation to civil transport aircraft", *NASA/CR*-1999-209338, pp.1-59.

Neuburger, D., Wygnanski, I., 1988, "The use of a vibrating ribbon to delay separation on two dimensional airfoils: Some preliminary observations", in Proc. Workshop II on Unsteady Separated Flow, ed. J.M. Walker, Frank J. Seiler Research Laboratory Report No.TR-88-0004.

Nishizawa,A., Takagi,S., Abe,H., Maeda,R., Yoshida,H., 2003, "Toward smart control of separation around a wing –Development of an active separation control system-", *Proc. 4th Symp. Smart Control of Turbulence*, Univ. Tokyo, March 2-4, pp.13-21.

Ozaki, Y., Ohyama, T. Yasuda, T. and Shimoyama, I., 2000, "An air flow sensor modeled on wind receptor hairs of insects", in Proc. MEMS 2000, Miyazaki, Japan, Jan. 23-27.

Takagi,S., Tokugawa, N., Yoshida, H., Abe, H., Atobe, T., Yamamoto, K., 2001, "Observation and control of separation from bluff bodies", *Proc. 2nd Symp. Smart Control of Turbulence*, Univ. Tokyo, March 4-6, pp.121-176.

Takagi,S., Tokugawa, N., Nishizawa, A., Abe, H., Kikushima, Y., Maeda, R., Yoshida, H., 2002, "Toward smart control of separation around a wing", *Proc. 3rd Symp. Smart Control of Turbulence*, Univ. Tokyo, March 3-5, pp.9-14.